

Study of an alkaline bath for tin deposition in the presence of sorbitol and physical and morphological characterization of tin film

R. L. BROGGI¹, G. M. DE OLIVEIRA¹, L. L. BARBOSA¹, E. M. J. A. PALLONE² and I. A. CARLOS^{1,*}

¹Departamento de Química, Universidade Federal de São Carlos, Via Washington Luiz, KM 235, CP 676, 13565-905, São Carlos, SP, Brazil

²Departamento de Engenharia de Materiais, UFSCar, São Carlos, SP, Brazil

(*author for correspondence: tel.: +55-16-3351-8206; fax: +55-16-3351-8350; e-mail: diac@power.ufscar.br)

Received 7 February 2005; accepted in revised form 18 October 2005

Key words: platinum electrode, sorbitol, tin electrodeposition, voltammetry

Abstract

Effects of sorbitol concentration on the deposition of tin on to platinum were studied by cyclic voltammetry. It was observed that sorbitol affected the tin-plating rate and also the thermodynamics of the deposition process. Rotating disk electrode studies showed that the deposition rate is controlled by mass transport and that the diffusion coefficient of the Sn(II) complex decreases with increasing sorbitol concentration. The presence of sorbitol in the plating bath was beneficial since a plating current efficiency of ~70% was obtained, while in its absence it was ~19%. Scanning electron microscopy showed that sorbitol works as a brightener since tin crystallites were much smaller than those obtained from alkaline solution in the absence of sorbitol. Also, at 1.0 M, sorbitol produced a very smooth film. X-ray spectra showed that β -Sn was deposited.

1. Introduction

The relevance of studying tin electrodeposition lies in its application in the electronic and food industries where good solderability and non-toxicity are important, respectively. The baths for tin electrodeposition are alkaline or acid. Tin acid baths (fluoboric, sulphate, chloride or methanesulfonic) [1–6] generally contain additives such as: naphtholsulfonic and cresolsulfonic acid to inhibit the oxidation of Sn(II) to Sn(IV) in solution and β -naphthol, gelatin, etc, as levellers [7]. The tin alkaline plating bath containing stannate $[\text{Sn}(\text{OH})_6]^{2-}$ has the advantage of not requiring additives since its deposition occurs at a very negative potential and the hydrogen evolution in parallel with tin deposition acts as a leveller [4]. However, the disadvantage is the diffusion of hydrogen inside the tin deposits. Whereas, tin deposits obtained from stannate are uniform, those obtained from stannite $(\text{HSnO}_2)^-$ are spongy and non-coherent [1–4, 7], showing the need for leveller additives in the plating baths. Also, another negative aspect of this bath is the oxidation of $(\text{HSnO}_2)^-$ by oxygen in solution to $(\text{SnO}_3)^-$.

Molenaar et al. [8] observed that polyalcohols inhibit the growth of tin crystals in tin autocatalytic deposition solution.

Previous studies in our laboratory on lead, copper, copper–zinc and copper–tin deposition processes

showed that sorbitol has brightening and leveling characteristics [9–12]. Encouraged by these findings we evaluated and analyzed the effect of sorbitol on the deposition process and morphology of the tin films. Cyclic voltammograms of plating solutions in the absence and presence of various sorbitol concentrations were investigated to elucidate the effect of additive on the deposition. Diffusion coefficients of the Sn(II) complex in the presence and absence of sorbitol were obtained through rotating disc electrode (RDE) studies. The morphology and structure of deposits were analyzed by scanning electronic microscopy (SEM) and X-ray diffraction, respectively.

2. Experimental details

The electrolyte used in all experiments was 3.0 M NaOH containing 0.10 M SnCl_2 , plus various sorbitol concentrations (0.15, 0.20, 0.30, 0.45 and 1.0 M). Analytical grade chemicals and double-distilled water were used. A Pt disk (0.196 cm²), a Pt plate and an appropriate Lugging capillary containing Hg/Hg₂Cl₂/KCl (1.0 M), were employed as working, auxiliary and reference electrodes, respectively. Where indicated, an Sn disk electrode (0.28 cm²) replaced the Pt disk electrode. Immediately prior to the electrochemical measurements, the working electrode was ground with 0.3 μm alumina

and rinsed with double-distilled water. Potentiodynamic measurements were performed with an EG&G model 366A bipotentiostat. Measurements of deposition and dissolution charges were made with an EG&G model 179 coulometer. All experiments were carried out at 25 °C. The current efficiency (ϕ_e) of tin electrodeposition was obtained from the stripping/deposition charge ratio. The tin films were obtained chronoamperometrically from 0.0 V to various deposition potentials (E_d), at a charge density (q_d) of 1.5 C cm⁻². The anodic stripping was done in 3.0 M NaOH. SEM micrographs were taken with an FEG X L 30. X-ray diffraction patterns were produced with filtered Cu-K α radiation (1.5406 Å), using a goniometer Rigaku Rotaflex RU200B. The diffraction experiments were in 2 θ scan mode with ω fixed at 2°.

3. Results and discussion

3.1. Electrodeposition of Sn on platinum in the presence of sorbitol

Figure 1 shows voltammograms for the stationary Pt substrate in the 0.1 M Sn²⁺ + 3.0 M NaOH plating bath at various sorbitol concentrations. The main feature of these voltammograms is the cathodic peak, characterized by a sharp increase in current density, after which the current density decreases less steeply, owing to mass-transport limitation. Moreover the tin-plating rate is affected kinetically by sorbitol concentration, since current density (j_p) magnitudes are significantly lower as sorbitol content rises, being highest in the absence of sorbitol. The fall in j_p in the presence of sorbitol is probably due to mass transport control of the deposition process, as can be seen later (Figure 6). Moreover, the presence of sorbitate anion in the double layer may hinder the discharge of stannite so that the system enters mass transport control sooner, leading to decreases in j_p . As a result of these processes, the morphology of the deposit is modified, as can be seen later in Section 3.2. The latter effect was observed during lead [9] and copper [10] electrodeposition from an alkaline plating bath in the presence of sorbitol, when inhibition of crystallite growth took place. These results are very significant since the presence of sorbitol in the deposition bath may lead to a better quality tin deposit than in its absence.

Also, it can be seen from Figure 1 that the presence of sorbitol leads to displacement of the deposition potential to more negative values than in its absence. This probably occurs because the sorbitol stabilizes the stannite anion by hydrogen bonds between sorbitol and the anion [8]. Thus, the breaking of these H-bonds at the metal–solution interface and the slow sorbitol diffusion and the corresponding changes in the composition of the solution layer near to the electrode contribute to high polarization. Moreover, it can be verified from Figure 1 that at higher sorbitol concentration E_d changes to more positive values, probably due to association among sorbitol molecules.

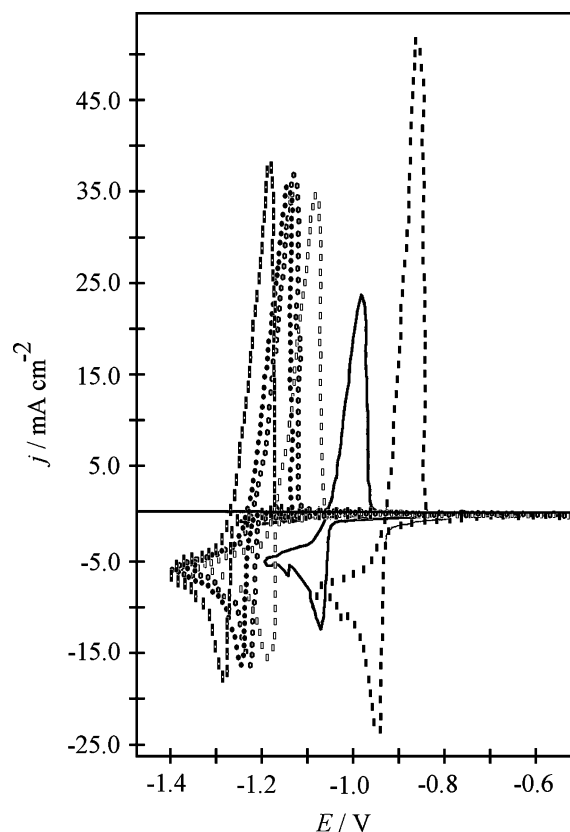


Fig. 1. Voltammograms for platinum substrate in 0.1 M Sn(Cl)₂ + 3.0 M NaOH at various sorbitol concentrations: (□) 0.0; (○) 0.15; (◐) 0.20; (◑) 0.30; (◒) 0.45 and (◓) 1.0 M, at 10 mV s⁻¹.

Then, stannite anions may be less stabilized by sorbitol, leading to discharge at less negative potential, i.e., -1.08 V for 1.0 M sorbitol. Also, at this additive concentration the plating bath showed significant viscosity, which decreases the mobility of the stannite–sorbitol complex [13].

The hydrogen evolution reaction (HER) region on platinum and tin electrodes was investigated further and the cathodic voltammograms for these substrates show no current up to approximately -1.0 and -1.8 V, respectively (Figure 2(a), (b)), suggesting that HER is the only significant competitive reaction in the initial part of the deposition process.

The presence of sorbitol proved to be very useful, since solutions are stable over time. Indeed, in its absence it was impossible to prepare stable solutions of stannite in 3.0 M NaOH. In the presence of sorbitate, stannite decomposition to SnO₂, caused by absorption of carbon dioxide from the air [1], was not observed, because sorbitol stabilizes Sn(II) in solution [8, 14, 15].

Figure 3 illustrates the effect of sorbitol concentration on the current efficiency (ϕ_e) of tin deposition. Tin films were obtained potentiostatically at various potentials and sorbitol concentrations in the plating bath, respectively, at charge density of -1.5 C cm⁻².

For sorbitol concentrations lower than 0.20 M, ϕ_e values decrease significantly as the Sn films did not totally cover the Pt substrate. Thus the contribution of HER to the deposition current is more significant,

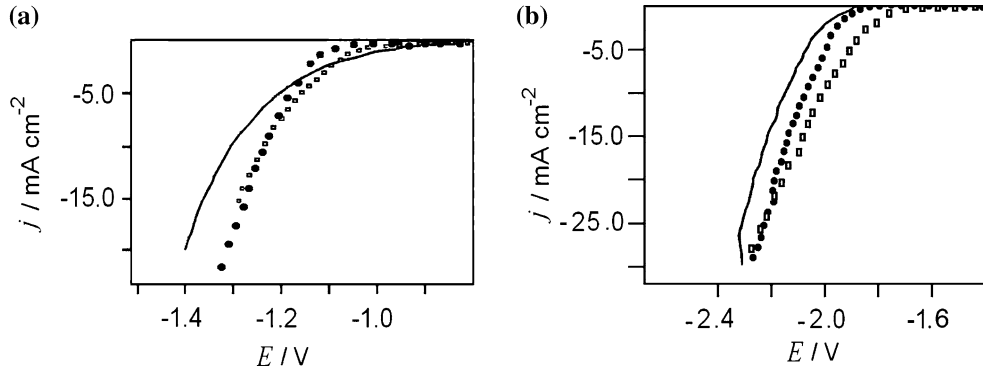


Fig. 2. Voltammetric curves for platinum (a) and tin (b) substrates from NaOH 3.0 M in the absence (—) and presence of sorbitol 0.15 M (●●) or 1.0 M (□□) at 10 mV s^{-1} . Potential values were referred to the calomel 1.0 M KCl electrode.

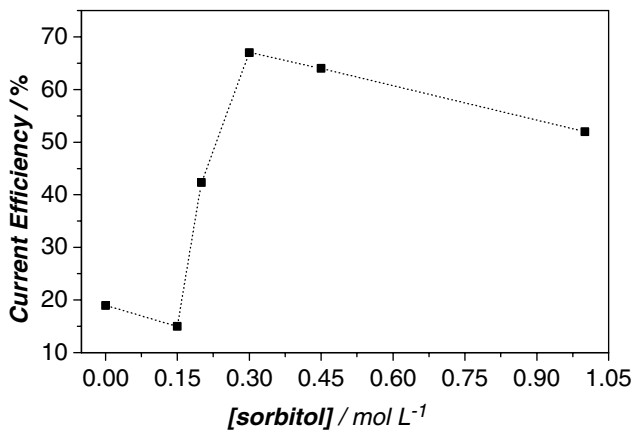


Fig. 3. Values of current efficiency (ϕ_e) as a function of sorbitol concentration $E_d = -0.97; -1.30; -1.26; -1.25; -1.21$ and -1.09 V and at charge density of -1.5 C cm^{-2} .

leading to low ϕ_e values. Also, for sorbitol concentrations higher than 0.20 M, ϕ_e values were $\sim 70\%$, due to the HER in the initial moments of the

deposition process, as can be seen better in Figure 2(a) and (b).

The plating bath containing 0.10 M $\text{SnCl}_2 + 3.0 \text{ M NaOH}$ and 0.3 M or 1.0 M sorbitol was chosen for subsequent studies.

The reverse sweep technique was applied during tin deposition from 0.10 M $\text{SnCl}_2 + 3.0 \text{ M NaOH}$ at a sorbitol concentration of 0.30 M (Figure 4). When the sweep was reversed at a potential of -1.26 V (Figure 4(a)), an increase in cathodic current and a crossover were observed, suggesting that the metal deposition occurred by 3D nucleation [16]. After the crossover, the cathodic current decreased quickly before the formation of an anodic peak. When the sweep was reversed at -1.30 V (broken line, Figure 4(b)) and at -1.45 V (dotted line, Figure 4(b)), the current decreased, indicating that the plating process was under diffusion control [13].

Figure 5(a) shows a set of voltammograms obtained at various sweep rates from a bath containing 0.10 M $\text{SnCl}_2 + 3.0 \text{ M NaOH}$ and 0.3 M sorbitol. The current

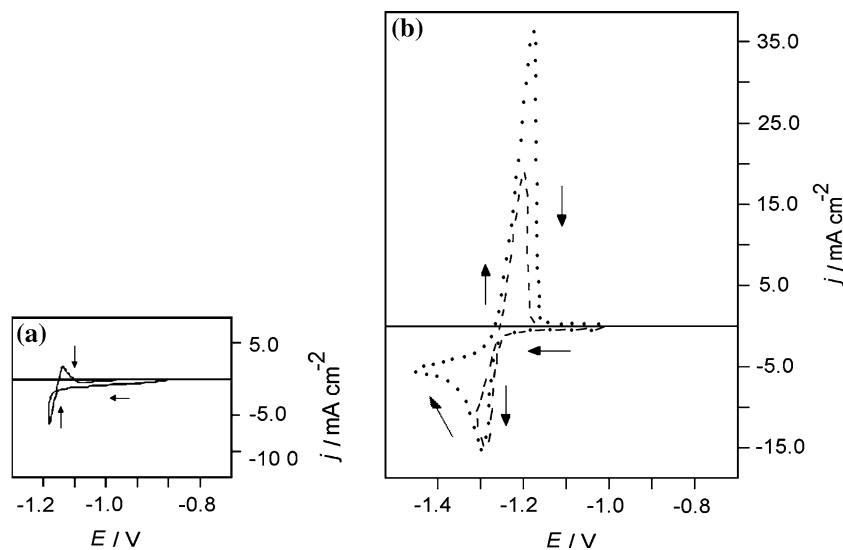


Fig. 4. Voltammetric curves for platinum substrates in 0.10 M $\text{SnCl}_2 + 3.0 \text{ M NaOH} + 0.3 \text{ M sorbitol}$; effect of the limit potentials: (a) (—) -1.26 V ; (b) (●●) -1.30 V and (□□) -1.45 V .

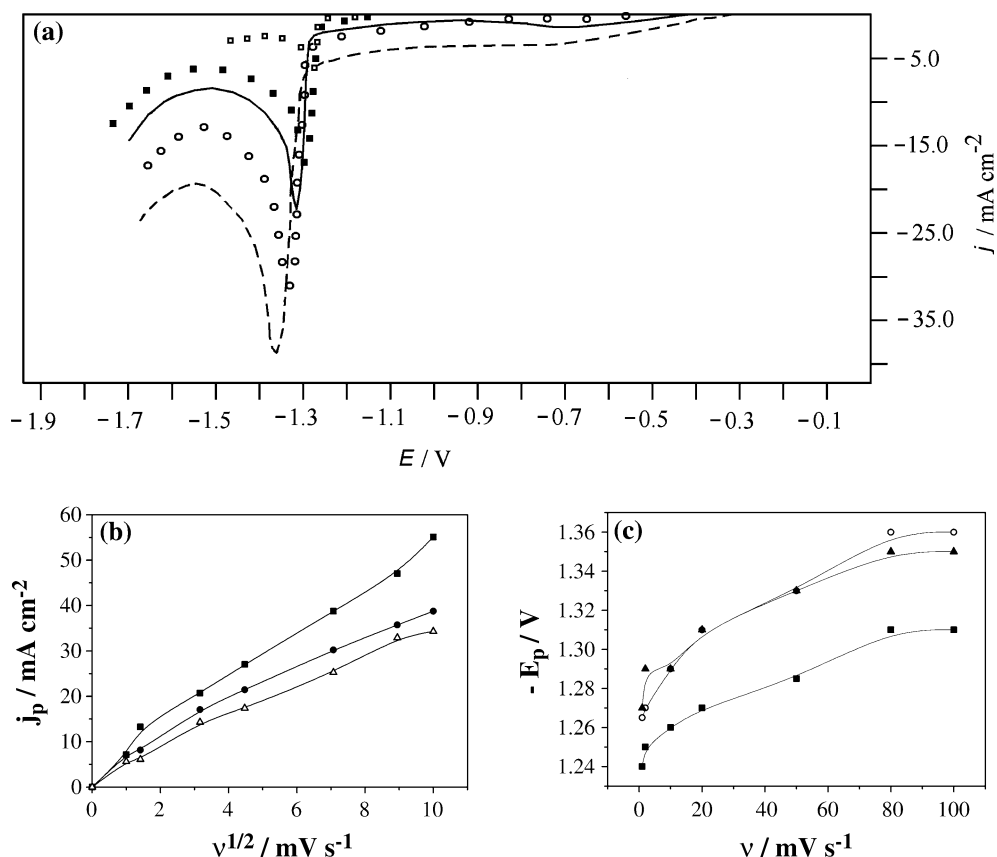


Fig. 5. Voltammetric curves for platinum substrate in 0.10 M $\text{SnCl}_2 + 3.0$ M NaOH (a) and 0.30 M sorbitol at various sweep rates ($v/\text{mV s}^{-1}$): (•••) 1.0; (••••) 10.0; (—) 20.0; (•••••) 50.0 and (---) 100.0. (b) Variation of j_p with $v^{1/2}$ at various sorbitol concentrations: (■) 0.0; (●) 0.30 and (△) 1.0 M. and (c) variation of E_p with v at various sorbitol concentrations: (■) 0.0; (○) 0.30 and (○) 1.0 M for tin electrodeposition.

density at the cathodic peak exhibits a steep increase with increasing sweep rate. It can be inferred from these voltammograms that the rate of tin deposition is probably controlled by mass transport. Figure 5(b) shows that peak current density (j_p) increases with $v^{1/2}$, but is not proportional, suggesting that the tin electrodeposition process is quasi-reversible in this region [13]. Figure 5(c) shows that peak potential (E_p) shifts negatively with increasing v , confirming the results of Figure 5(b). Similar results to Figures 4 and 5(a)–(c) were obtained from the tin-plating bath containing 1.0 M sorbitol.

To confirm the results obtained with the stationary electrode concerning the mass transport control of the deposition process, studies with a rotating disk electrode (RDE) were made from Sn plating baths in the absence and presence of 0.3 M and 1.0 M sorbitol. Figure 6 shows that limit current densities (j_L) increase with $f^{1/2}$. These results corroborate those obtained in Figure 5, since deposition current densities are dependent on the speed of rotation. The diffusion coefficient (D_0) of the tin complex in the presence of the 0.3 M and 1.0 M sorbitol and in the absence of sorbitol was obtained from these RDE studies. Assuming a kinematic viscosity of $0.01 \text{ cm}^2 \text{ s}^{-1}$, and a roughness factor of ~ 2.0 (Pt substrate) [12, 17, 18], the value of the diffusion coefficient was $1.84 \times 10^{-6} \text{ cm}^2 \text{ s}^{-1}$ in the absence of additive and $0.83 \times 10^{-6} \text{ cm}^2 \text{ s}^{-1}$ and

$0.55 \times 10^{-6} \text{ cm}^2 \text{ s}^{-1}$ for 0.3 M and 1.0 M sorbitol, respectively. The latter values, as expected, are smaller than for the stannite ion. This is because the size of the stannite–sorbitol complex is greater than that of the stannite ion, and consequently the former has lower mobility. Also, the increase in viscosity due to addition of sorbitol contributed to the decrease in D_0 .

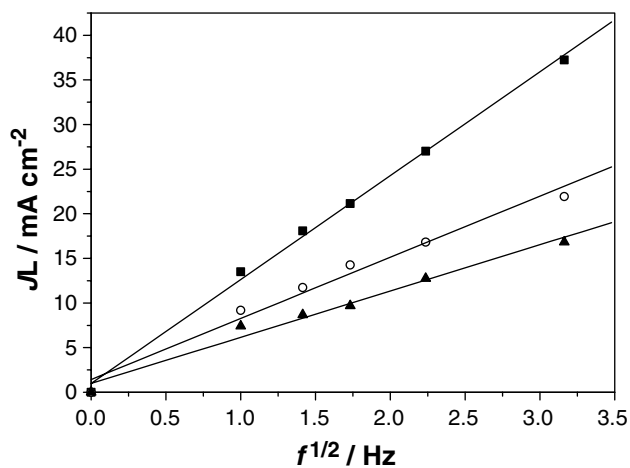


Fig. 6. Curves of density of limit current vs. $f^{1/2}$ for tin electrodeposition on to platinum substrate in 0.10 M $\text{SnCl}_2 + 3.0$ M NaOH and concentration different of sorbitol: (■) 0.0; (○) 0.30 and (▲) 1.0 M.

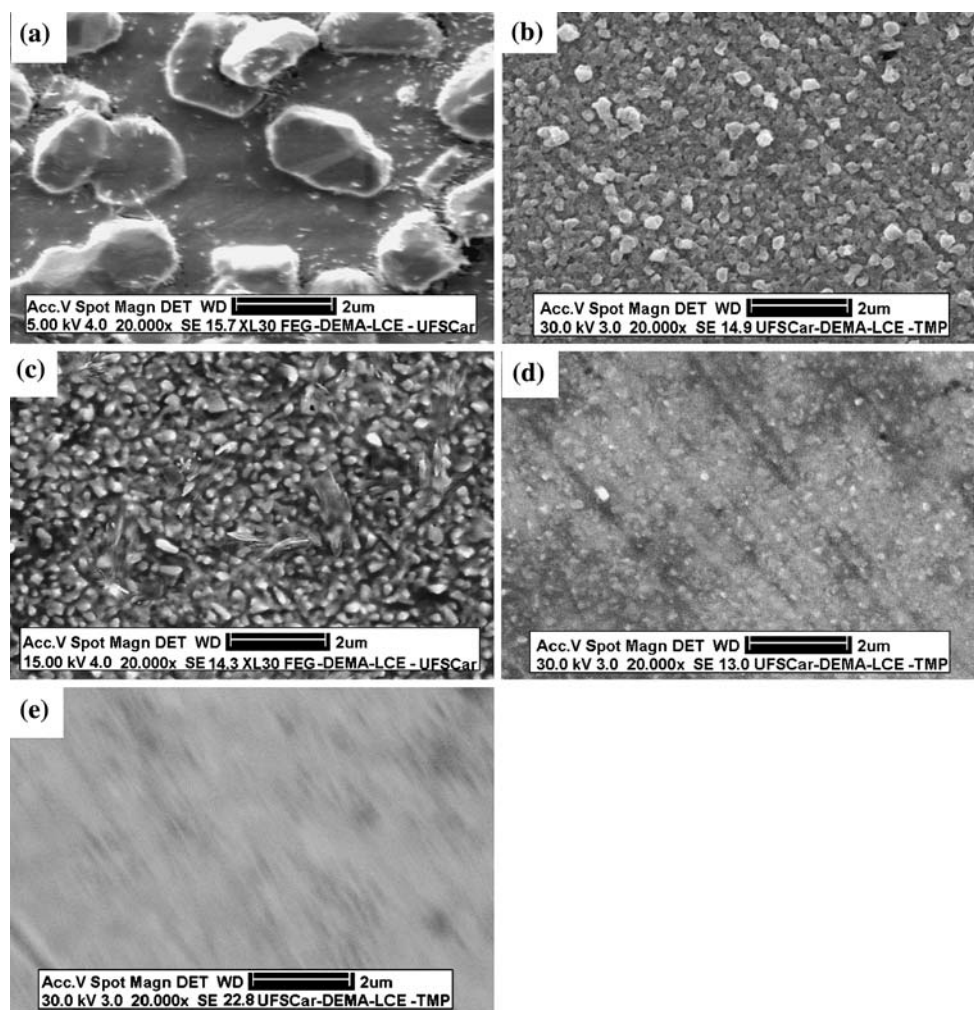


Fig. 7. SEM micrographs of Sn films obtained at various E_d : (a) -0.97 V; (b) -1.30 V; (c) -1.26 V; (d) -1.25 V and (e) -1.09 V at $q_d = 1.5 \text{ C cm}^{-2}$. Electrolytic solutions $0.1 \text{ M SnCl}_2 + 3.0 \text{ M NaOH}$ and at various sorbitol concentrations: (a) absence; (b) 0.15 M ; (c) 0.2 M ; (d) 0.3 M and (e) 1.0 M .

Finally, it can be verified from the potentiodynamic curves for the platinum electrode in the Sn baths in the presence of sorbitol that initial deposition rates are high, but lower than in its absence (Figure 1). As a consequence, deposits with refined crystallites occur and also, at a certain sorbitol concentration, smoothing can occur, as seen later (Section 3.2).

3.2. Morphological study of tin film

Figure 7(a)–(e) shows SEM micrographs of Sn films formed from solution containing $0.1 \text{ M SnCl}_2 + 3.0 \text{ M NaOH}$ in the absence and presence of various sorbitol concentrations and at a charge density of 1.5 C cm^{-2} and various deposition potentials. As sorbitol concentration increases, the size of Sn crystallites decreases. Moreover, for 1.0 M sorbitol the Sn films are smooth. These results indicate that Sn deposition from an alkaline bath containing sorbitol leads to better quality deposits, since sorbitol acts as a brightener.

3.3. X-ray analysis of the Sn film

Figure 8 shows typical X-ray diffraction patterns of some deposits. The observed crystallographic distances, d_{obs} : d_1 (hkl), d_2 (hkl) and d_3 (hkl) are compared with expected values (d_{exp}) described in JCPDS [19] in Table 1. Some diffraction lines were easily assigned to $d(\text{Pt})$, SnPt_3 and $d(\beta\text{-Sn})$. Also, it is possible that tin oxides (SnO) were produced during the electrodeposition of the Sn films.

4. Conclusions

Sn alkaline plating baths were successfully obtained with sorbitol as an additive since the solution was stable and bath decomposition was not observed during the deposition. From cyclic voltammograms it was verified that sorbitol affects both the kinetics and the thermodynamics of the deposition process, decreasing the tin-plating rate and shifting the deposition potential

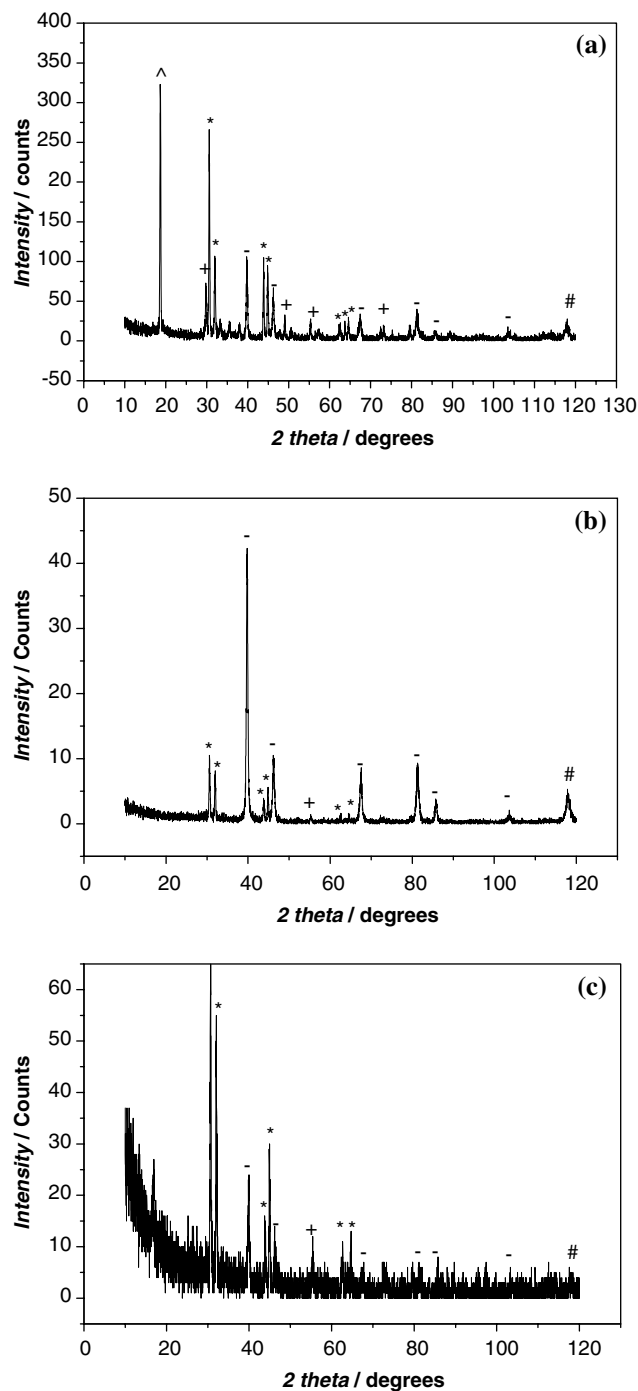


Fig. 8. X-ray diffraction patterns of deposits obtained from SnCl_2 0.1 M + NaOH 3.0 M in: (a) 0.0 M; (b) 0.3 M and (c) 1.0 M sorbitol, at different potentials -0.97 V, -1.25 V and -1.09 V, respectively, and a charge density of 1.5 C cm^{-2} . Potential values were referred to the calomel 1.0 M KCl electrode. β -Sn (*, JCPDS – 04-0673); SnPt_3 (#, JCPDS – 35-1360); SnO (+, JCPDS – 24-1342); Sn_3O_4 (^, JCPDS – 20-1293); Pt (-, JCPDS – 04-0802).

to more negative values. The electrochemical efficiency of Sn deposition was $\sim 70\%$ in the presence of sorbitol, while in its absence it was $\sim 19\%$. An increase in current was observed when the Sn deposition voltammetry was reversed in the initial moments of the process, suggesting 3D nucleated deposition in this region. Hydrodynamic studies of Sn deposition showed that the deposition process is controlled by mass transport and that the

diffusion coefficient is 1.84×10^{-6} (absence of sorbitol), 0.83×10^{-6} and $0.55 \times 10^{-6} \text{ cm}^2 \text{ s}^{-1}$ for 0.3 M and 1.0 M sorbitol in the plating bath, respectively. SEM analysis showed that the presence of sorbitol leads to high quality films which totally coat the substrate and for 1.0 M sorbitol, are smooth. The X-ray analysis of the Sn films obtained in the absence and presence of sorbitol indicated the occurrence of β -Sn.

Table 1. Observed interplanar distances, $d(hkl)$, of X-ray diffraction patterns of tin deposits obtained at (E_d): (a) -0.97 V, (b) -1.25 V and (c) -1.09 V, with $q_d = 1.50$ C cm $^{-2}$, from various baths: (a) 0.0 M Sorbitol, (b) 0.3 M Sorbitol and (c) 1.0 M Sorbitol

d_1 (hkl) (a)	d_2 (hkl) (b)	d_3 (hkl) (c)	$d_{\text{exp}}(\beta\text{-Sn})$	$d_{\text{exp}}(\text{SnPt}_3)$	$d_{\text{exp}}(\text{SnO})$	$d_{\text{exp}}(\text{Sn}_3\text{O}_4)$	$d_{\text{exp}}(\text{Sn}_2\text{O}_3)$	$d_{\text{exp}}(\text{Pt})$	$d_{\text{exp}}(\text{SnO}_2)$
4.76					4.852 (10)	4.842 (30)			
2.99					2.990 (100)				2.985 (100)
2.92	2.92	2.92	2.916 (100)		2.901 (80)	2.917 (35)			
2.79	2.79	2.79	2.794 (90)		2.781 (80)	2.794 (30)	2.774 (25)		
2.26	2.26	2.26		2.254 (30)			2.256 (12)	2.266 (100)	
2.06	2.06	2.06	2.063 (34)				2.068 (1)		
2.02	2.01	2.01	2.019 (74)	2.014 (50)	2.020 (40)	2.646 (50)			
1.96	1.96	1.96		1.967 (20)	1.961 (30)			1.962 (53)	
1.85					1.800 (10)		1.850 (2)		
1.65	1.65	1.65	1.659 (17)		1.660 (50)		1.649 (12)		
1.48	1.48	1.48	1.484 (23)						
1.45			1.458 (13)						
1.44	1.44	1.44	1.442 (20)						
1.38	1.38	1.38			1.382 (20)			1.387 (31)	
1.29			1.292 (15)		1.297 (20)				
1.18	1.18	1.18			1.175 (6)			1.182 (33)	
1.13	1.13	1.13						1.132 (12)	
0.98	0.98	0.98	0.982 (5)		0.985 (2)			0.981 (6)	
0.90	0.90	0.90		0.895 (35)				0.900 (22)	

The expected values are from JCPDS [19]. Potential values were referred to the calomel 1.0 M KCl electrode.

d_{obs} : $d_1(\text{hkl})$; $d_2(\text{hkl})$ and $d_3(\text{hkl})$.

Acknowledgements

Financial support from the Brazilian agency CAPES and FAPESP are gratefully acknowledged.

References

1. F. Lowenheim, *Modern Electroplating*, 3rd ed., (John Wiley and Sons, New York, 1974).
2. Tin Research Institute. Instruction for Electrodepositing Tin, 5th ed., 1979. in T.M.C. Nogueira, Ph.D. Thesis, Universidade Federal de São Carlos, Brazil (1996).
3. Hirsch S. Tin-lead, lead and tin plating. Special Metal Finishing-Guide and Directory Issue. **93**(1A) (1995) 304.
4. J.P. Nityanandan and H.V.K. Udupa, *Metal Finish* **July** (1973) 44.
5. C. Rosenstein, *Metal Finish* **January** (1990) 17.
6. G.A. Federman, Annals of 5th International Tinplate Conference, London, England (1992) 88.
7. T.M.C. Nogueira, Ph.D. Thesis, Universidade Federal de São Carlos, Brazil (1996).
8. A. Molenaar and J.W.G. de Bakker, *J. Electrochem. Soc.* **136** (1989) 378.
9. J.L.P. Siqueira, I.A. Carlos, M.R.H. Almeida and G.A. Finazzi, *J. P. Sources* **5185** (2003) 1.
10. L.L. Barbosa, M.R.H. de Almeida, R.M. Carlos, M. Yonashiro, G.M. Oliveira and I.A. Carlos, *Surf. Coat. Technol.* **192** (2005) 145.
11. I.A. Carlos and M.R.H. de Almeida, *J. Electroanal. Chem.* **562** (2004) 153.
12. G.A. Finazzi and I.A. Carlos, *Surf. Coat. Technol.* **187** (2004) 377.
13. A.J. Bard and L.R. Faulkner, *Electrochemical Methods: Fundamentals and Applications* (John Wiley and Sons, New York, 1980).
14. R.L. Broggi, L.L. Barbosa, I.A. Carlos, G.M. Oliveira and J.L.P. Siqueira, XIV Simpósio Brasileiro de Eletroquímica e Eletroanalítica, Teresópolis – RJ, Brazil, 2004 (CD-ROM).
15. R.L. Broggi, L.L. Barbosa, I.A. Carlos and G.M. Oliveira, Sociedade Brasileira de Química and XXVI Congresso Latino-americano de Química, Salvador – BA, Brazil, 2004 (CD-ROM).
16. S. Fletcher, C.S. Halliday, D. Gates, M. Westcott, T. Lwin and G. Nelson, *J. Electroanal. Chem.* **159** (1983) 267.
17. T. Biegler, D.A.J. Rand and R.W. Woods, *J. Electroanal. Chem.* **29** (1971) 269.
18. G.M. Oliveira, L.L. Barbosa, R.L. Broggi and I.A. Carlos, *J. Electroanal. Chem.* **578** (2005) 151.
19. Joint Committee on Powder Diffraction Standards (JCPDS) in International Centre for Diffraction Data. Powder Diffraction File- PDF-2. Database Sets 1–49. Pennsylvania, ICDD, 2000, (CD-ROM).